Available online at www.sciencedirect.com
ScienceDirect
Advances in Space Research 47 (2011) 2152–2161
ADVANCES IN SPACE RESEARCH (a COSPAR publication)
www.elsevier.com/locate/asr

Specification of the Earth's plasmasphere with data assimilation

A.M. Jorgensen [a,*], D. Ober [b], J. Koller [c], R.H.W. Friedel [c]

[a] New Mexico Institute of Mining and Technology, 801 Leroy Place, Socorro, NM 87801, USA
[b] AFRL/RVBXP, 29 Randolph Road, Hanscom AFB, MA 01731, USA
[c] Space Science and Applications, ISR-1, MS D466, Los Alamos National Laboratory, Los Alamos, NM 87545, USA

Received 6 April 2009; received in revised form 30 May 2010; accepted 6 June 2010
Available online 12 June 2010

Abstract

In this paper we report on initial work toward data assimilative modeling of the Earth's plasmasphere. As the medium of propagation for waves which are responsible for acceleration and decay of the radiation belts, an accurate assimilative model of the plasmasphere is crucial for optimizing the accurate prediction of the radiation environments encountered by satellites. On longer time-scales the plasmasphere exhibits significant dynamics. Although these dynamics are modeled well by existing models, they require detailed global knowledge of magnetospheric configuration which is not always readily available. For that reason data assimilation can be expected to be an effective tool in improving the modeling accuracy of the plasmasphere. In this paper we demonstrate that a relatively modest number of measurements, combined with a simple data assimilation scheme, inspired by the ensemble Kalman filtering data assimilation technique does a good job of reproducing the overall structure of the plasmasphere including plume development. This raises hopes that data assimilation will be an effective method for accurately representing the configuration of the plasmasphere for space weather applications.

Keywords: Kalman filtering; Plasmasphere modeling; Space weather; Data assimilation

1. Introduction

Data assimilation techniques are widely used in weather forecasting and that is perhaps the field in which they are most well known (e.g. Kalnay et al., 1998). However, data assimilation techniques are used in one form or another in a wide variety of data estimation problems. Other examples include radar tracking problems (e.g. Ramachandra, 2000). Data assimilation works by merging, by any means, a model which is a physical description of a system with measurements which constrain the state or evolution of the system in some relevant way. The free model parameters are then adjusted to maximize the agreement between the model and the measurements.

One of the most effective data assimilation methods is the Kalman filter (Kalman, 1960), with early applications to radar tracking problems. The original approach developed by Kalman required all the derivatives of the model with respect to adjustable parameters, such that for very large problems or complex non-linear models this became cumbersome. Several alternatives, some based on statistical approximations, were developed. Among them the ensemble Kalman filter (Evensen, 2003) is now widely used in weather prediction, and does not require derivatives. Instead it requires the model to be run many times with different parameters in order to sample parameter space statistically.

In recent years Kalman filtering techniques have been applied to space weather prediction problems, particularly to the prediction of the radiation belts, with good success (Koller and Friedel, 2005; Koller et al., 2007; Maget et al., 2007; Kondrashov et al., 2007; Naehr and Toffoletto, 2005; Rigler et al., 2004). These projects aim to provide a complete specification of the radiation belts based on satellite measurements and a good but imperfect physics-based model. The work by Koller uses the Rasmussen and Schunk (1990), Rasmussen et al. (1993) plasmasphere model, but

* Corresponding author. Tel.: +1 575 835 5450.
E-mail address: anders@nmt.edu (A.M. Jorgensen).

0273-1177/$36.00
doi:10.1016/j.asr.2010.06.013

does not close the data assimilation loop around the model, relying instead on solar wind parameters to drive the model. The plasmasphere is a region of dense plasma trapped in the co-rotating portion of the inner magnetosphere. Plasmasphere dynamics is driven by ionospheric sources and sinks, and by the changing magnetospheric electric field, which with the magnetic field combine to create density gradients and plasma plumes (e.g. Lemaire and Gringauz, 1998; Darrouzet et al., 2009). The plasmasphere is a significant driving force on the radiation belts as regions of large density gradients host the waves responsible for acceleration and loss of radiation belt particles (e.g. Friedel et al., 2002; Horne and Thorne, 1998).

In this paper we report on initial work to develop a data assimilative approach to modeling the plasmasphere. We use the plasmasphere model by Ober et al. (1997) and a ensemble data assimilation approach inspired by ensemble Kalman filtering. We use a real interval of K_P to simulate the plasmasphere and generate simulated data, which we then input to the data assimilation method in an attempt to recover the plasmasphere configuration and the input K_P.

The Ober et al. (1997) model is a physics-based model of the plasmasphere. The overall operation of the model can be described in three simple equations: one equation which describes the dayside outflow from the ionosphere, containing two free parameters, the plasmasphere saturation density and the maximum outflow rate; one equation which describes the nightside inflow to the ionosphere, containing one free parameter, the decay rate; and one equation which describes convection and continuity. In addition, the model takes as inputs arbitrary electric and magnetic fields. For the purpose of this paper we use a dipole magnetic field and an electric field which is parametrized by K_P (Sojka et al., 1986).

2. Methodology

In this paper we employ a simpler data assimilation approach than ensemble Kalman filtering because of the ease with which it can be implemented. We use the Ober et al. (1997) plasmasphere model, which is written in the Fortran language. We wrote a C-language wrapper which allows us the necessary access to the model internals. This includes the ability to read and write the plasma density map between the model and a storage array, the ability to simulate satellite density measurements from the plasma density map, and the ability to set the external parameter (in this case K_P) and run the model for a fixed time interval as a subroutine. This is illustrated in Fig. 1(a).

The data assimilation approach which we use involves an ensemble of models similar to ensemble Kalman filtering. However, for the purpose of simplicity we run each model in the ensemble at a fixed K_P. At each data assimilation time, where data and models are compared, the best model is selected and its density map is copied to all the other running models.

The assimilation procedure is thus as follows. Several models are run in parallel from the same initial condition with different values of K_P for a fixed interval of time (in reality the different models are run serially on a single processor, and the plasma density maps and model parameters are copied in and out of the model for each). At the end of the interval satellite density measurements are simulated from each model and compared with the input data. The cost function for this comparison is the sum of squares of fractional errors. The plasma density from the best model is then copied to each of the running models, and the models are then run again for another fixed interval of time. This is illustrated in Fig. 1(b).

This approach is significantly simplified compared to for example ensemble Kalman filtering (e.g. Evensen, 2003). In ensemble Kalman filtering the full probability distribution is approximated by an ensemble, and formal errors are derived. In our approach, which is an initial test, for the sake of simplicity, we only track the best-fitting model amongst an ensemble of fixed drivers. The success of this simple approach will inform whether more sophisticated modeling approaches are warranted.

In this paper we work with simulated data, which are generated from a period of real K_P values in order to have realistic plasma density variations. We use the first half of December 2006, whose K_P values are plotted in Fig. 2. We simulate data for eight satellite orbits, including four elliptical orbit satellites and four geostationary satellites space evenly in local time as show in Fig. 3. We call these simulated data the input data. We do not simulate noise or any systematic effects on the data, but those are factors which must be considered in the future.

Fig. 4 shows a close look at several consecutive assimilation steps for a short interval of 4 h with data assimilation taking place every hour. In the figure the red curve is the input data, the blue curves each of the models run with different values of K_P (in this case the 11 values from 0 to 10), and the green curve represents the best model as determined by best agreement between the model and all satellites at the assimilation times, marked by the dotted lines. In this case the assimilation interval is 1 h. Notice that at the beginning of each hour all 11 models begin at the same point, and then diverge as time progresses because of the differing values of K_P. Although it appears that at 21 UT the assimilation did not pick the best-fitting model we should remember that this figure shows only one satellite out of eight.

Throughout this paper we use the 1-h assimilation interval, and run either 11 or 31 models in parallel, with K_P values evenly distributed in the [0; 10] interval. These are not the same values as used to generate the simulation from which the input data are derived. Those follow the encoding of K_P-values, 0, 0.3, 0.7, 1, 1.3, etc. We should note that although real K_p only covers a discrete set of values in the [0; 9] interval, the model is defined on a continuous variable and still produces a reasonable convection pattern outside of these discrete values, as well as in the [9; 10] interval. We do not expect the assimilation to make much use of values above 9, but give it access to this range of parameter

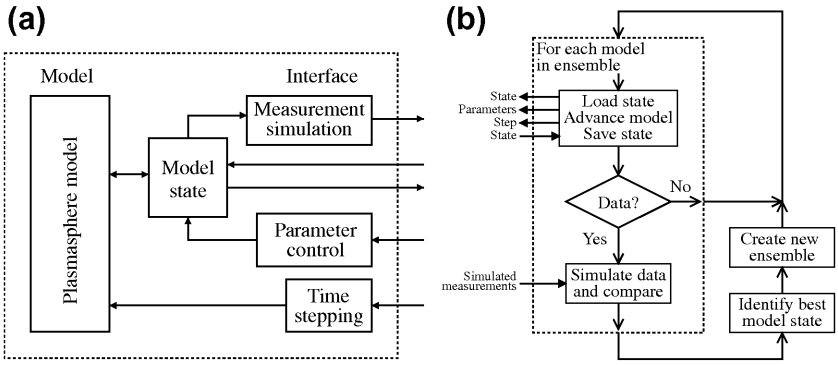

Fig. 1. Implementation of the simulation. (a) We interfaced the Ober et al. (1997) plasmasphere model (written in Fortran) with a C-language wrapper which provided access to reading and writing the plasma density and other model parameters. (b) This model is then included in the data assimilation loop, computing the plasma density for multiple models in parallel.

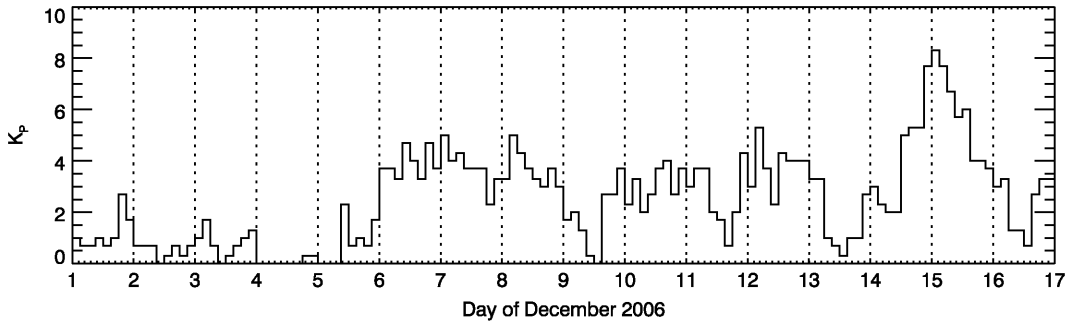

Fig. 2. K_P for the first 16 days of December 2006. This interval is used for the simulations because of the very quiet period at the beginning of the interval (days 1–5), the very active period (days 14–16), and the period of variable intermediate K_P (days 6–13).

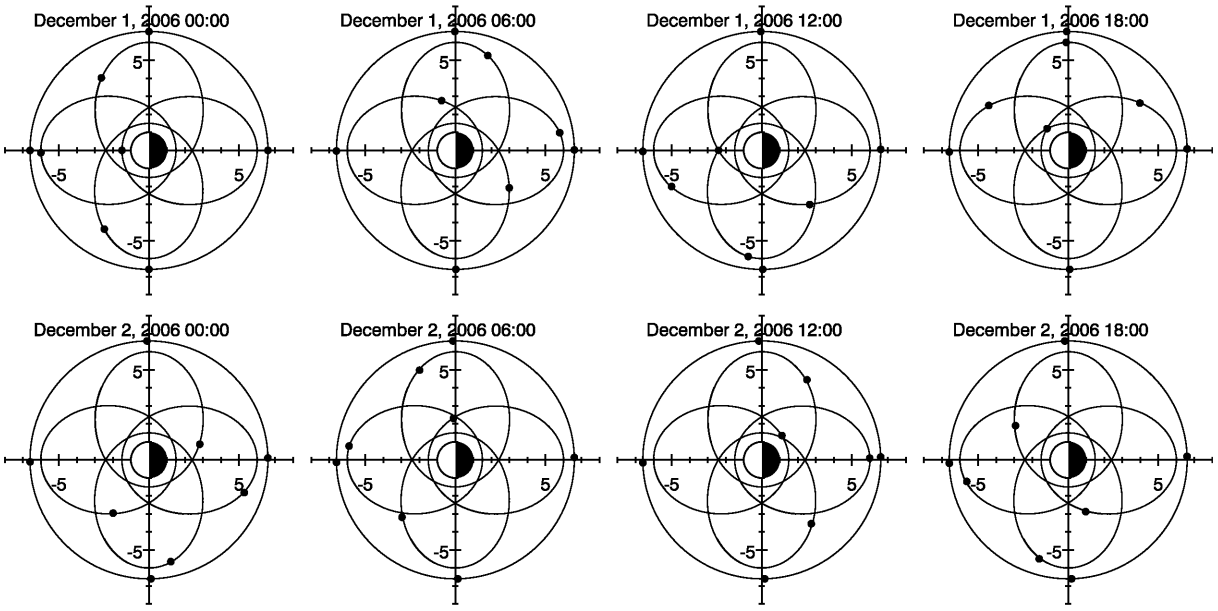

Fig. 3. Orbital positions of the eight satellites at 6-h intervals for the first 2 days of December 2006.

space anyway. A comparison of the real K_p and this parameter, selected by the assimilation, which we call "recovered K_p" is a reasonable measure of the performance of the assimilation.

3. Simulation results

We will report on four different simulations. The first simulation covers the first 16 days of December 2006 using

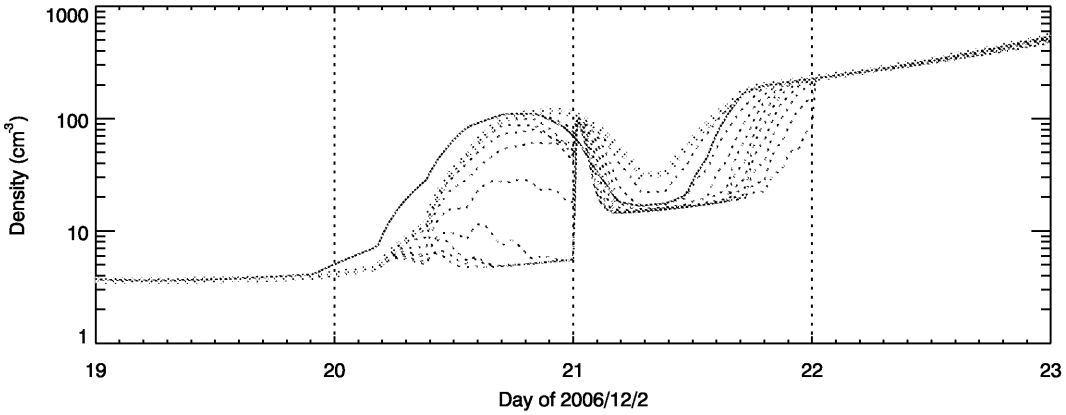

Fig. 4. Demonstration of the data assimilation method for a short interval on December 2, 2006. The red (solid) curve shows the satellites measurement, the blue (thin dotted) curves show the different assimilation attempts, whereas the green (thick dotted) curve shows the best assimilation attempt. The state is reset to one best matching the satellite measurements at the beginning of each hour. (For interpretation of the references to colour in this figure legend, the reader is referred to the web version of this article.)

11 parallel models and all eight satellites. In the second simulation we use 31 models and all eight satellites, whereas in the last two simulations we use 11 models and either the elliptical or geostationary orbit satellites.

3.1. 16-Day simulation

The results of this assimilation run are shown in Figs. 5–7. Figs. 5 and 6 (respectively, first and last 8 days of the assimilation) show the input plasma density actually measured by the satellites (in red) as well as the plasma density simulated by each of the parallel model runs (in blue). The green curve shows the plasma for the model which fit the data best at the hourly assimilation times. This is the same formatting scheme as shown in Fig. 4. The top four panels show the elliptical satellites, the next four panels the geostationary satellites. The last panel shows K_P, which is the only free parameter in the assimilation. The red curve shows the K_P used to generate the input data. The green curve shows the K_P of the best model for each hour interval, and the blue curve shows a double 5-h smooth of the green curve (double in order to produce a continuous second derivative and a nicer look).

Fig. 7 shows the density maps at 8-h intervals beginning at 8 UT on December 1, 2006. On each day the original simulation (on top) is compared with the recovered map (on the bottom). In general we observe the expected behavior of the plasmasphere. The plasmasphere is approximately circular with a slight bulge on the dusk side. During times of increasing activity (for example December 1 and 14 at 24:00) a pronounced plume extends to the dayside as dense plasma on newly open field lines drifts to the dayside magnetopause. At times when the activity level is decreasing the plume is located on the dusk side and is less pronounced, with plasma flowing generally from the area of the dusk side bulge toward the dayside magnetopause. As activity levels increase and decrease in rapid succession these behaviors result in more complicated plasmapause shapes.

In Figs. 5 and 6 there is generally good agreement between the input plasma density measurements and the best assimilated plasma density measurements. The first 2 days (December 1–2), and last 3 days (December 14–17) of the simulation fit particularly well, with even quite complex structure between 14 UT and 20 UT on December 2 being reproduced well. By contrast the interval from December 3 to 6 and even part of December 7 is not very well reproduced at all. The rest of the time the plasma density is reproduced quite well although there is a slight tendency for the assimilation step to place the plasmapause closer to the Earth than indicated by the input data.

In the K_P data (the last panel in Figs. 5 and 6) we see a similar pattern. Excellent agreement between input and recovered K_P on December 1, 2, 14, 15, and 16, very poor agreement on December 3–6 or 7, and good agreement the rest of the time, with a slight tendency towards a higher K_P than prescribed in the input data.

In the images (Fig. 7) the situation is again similar. On December 1 and 2 (first 6 columns of images of top 2 rows) the agreement between the recovered plasma density (top row) and the input density (second row) is excellent, with even fine plume structure being reproduced well. On December 3, 4, 5, and 6, the recovered and input plasma density are wildly different, with the recovered showing a much smaller plasmapause in agreement with the satellite density measurements in Fig. 5, and in agreement with the larger K_P that was selected during that time interval. On December 7, the recovered and input plasma density maps begin to look more similar, and generally agree well after that time except for a few differences, for example at 0 UT on December 12.

It is also interesting to note that during most of the simulation the recovered value of K_P (green curve in the last panels of Figs. 5 and 6) varies widely from hour to hour while its average (blue curve) is in much better agreement with the input K_P value. A likely explanation for this is that because none of K_P values available to the assimilation exactly match the input K_P, the assimilation compensates

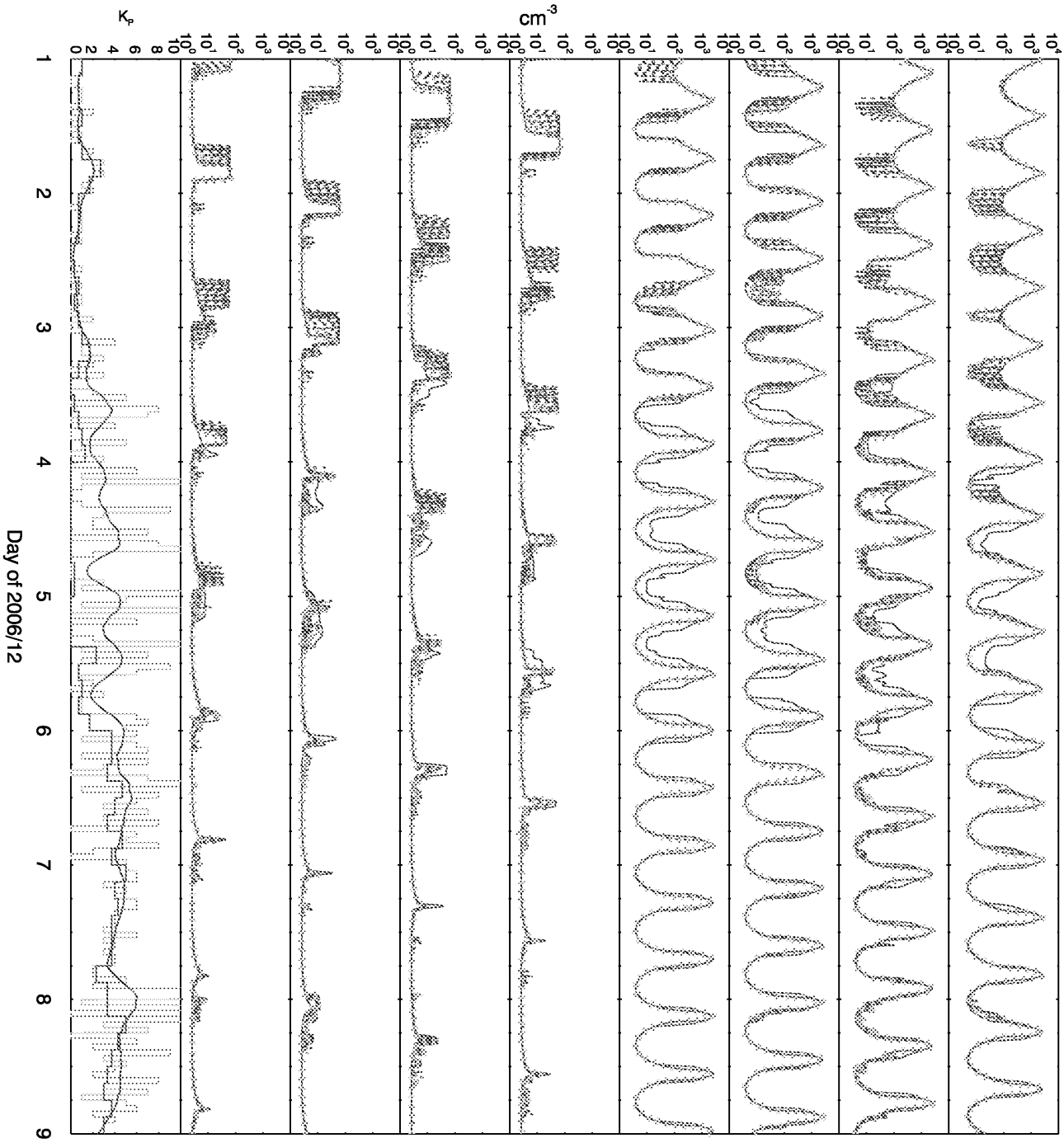

Fig. 5. Satellite density measurements for the first 8 days of December 2006. Panels (a)–(d) show elliptical satellite measurements. Panels (e)–(h) show geostationary satellite measurements. Panel (i) shows K_P. In each of panels (a)–(h) the red (solid) curve represents the simulated satellite measurements, whereas the blue (narrow dotted) curves represent the simulated density measurements from each of the ensembles, and the green (wide dotted) curve represents the best-fitting ensemble member. In the bottom panel the red curve (at 3 h interval) represents the real K_P value, from Fig. 2, the green curve (at 1 h interval) represents the K_P value selected by the assimilation, and the blue curve (smooth) represents the green curve smoothed twice with a 5-h boxcar window. (For interpretation of the references to colour in this figure legend, the reader is referred to the web version of this article.)

for this by selecting K_P values which are greater than and smaller than the input K_P to match the plasma density. It is however surprising that much of the time the swings are so great even though the average agrees well with the input K_P.

We do not know the reason why the assimilation began selecting very large values of K_P for a few days beginning on December 3. One possible explanation is that the satellites may have been positioned such that a number of the satellites would not distinguish between different values of K_P (i.e. measurements would look the same regardless of K_P), and the few that were able to distinguish had similar responses to both large K_P (possible plume formation) and small K_P (possible refilling of a large plasmasphere).

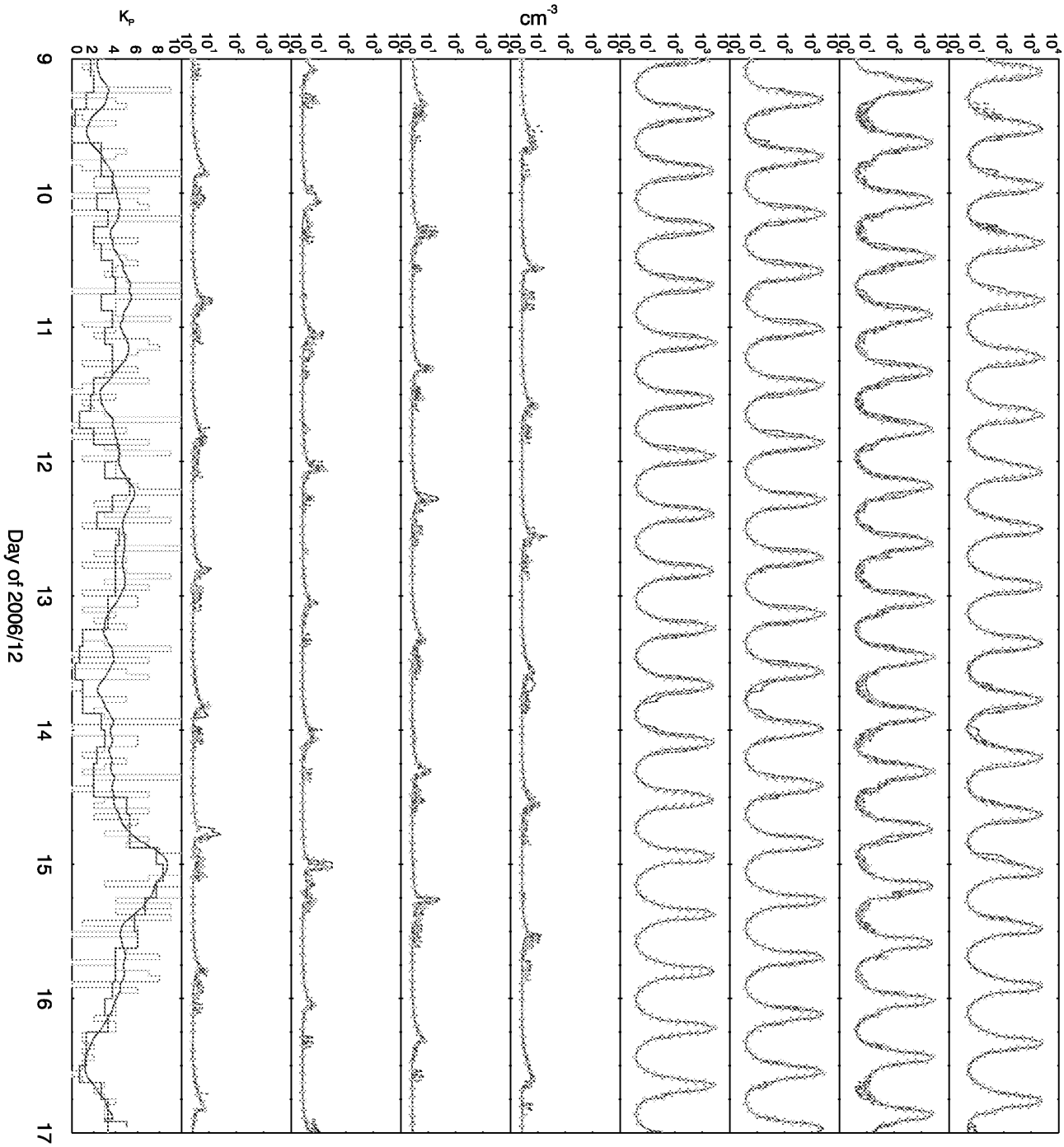

Fig. 6. Satellite density measurements for the second set of 8 days of December 2006. The plot format is identical to that of Fig. 5.

Because the assimilation does not use time history it may not be simple to distinguish the different options for K_P, and thus the choice is based on random noise. This in turn starts the plasmasphere down a irreversible path from which it takes several days to recover.

Also, it should be noted that on the second elliptical satellite there is a slightly larger spread of the blue curves. This could indicate that the position of that satellite is slightly better suited for distinguishing short-term variations of the plasmasphere. This satellite has perihelion on the dusk side and appehelion on the dawn side.

3.2. Increasing the number of assimilation states

Next we ask the question whether increasing the number of parallel simulations (and thus the number of parameter values) explored will improve the accuracy of the assimilation. In Fig. 8 we plot the value of K_P for the first 4 days of December 2006. The upper two panels show density, the lower two panels K_P values, both in the same format as described earlier. The first and third panel are for 11 assimilation states, whereas the second and fourth are for 31 assimilation states. It is clear from this that increasing the

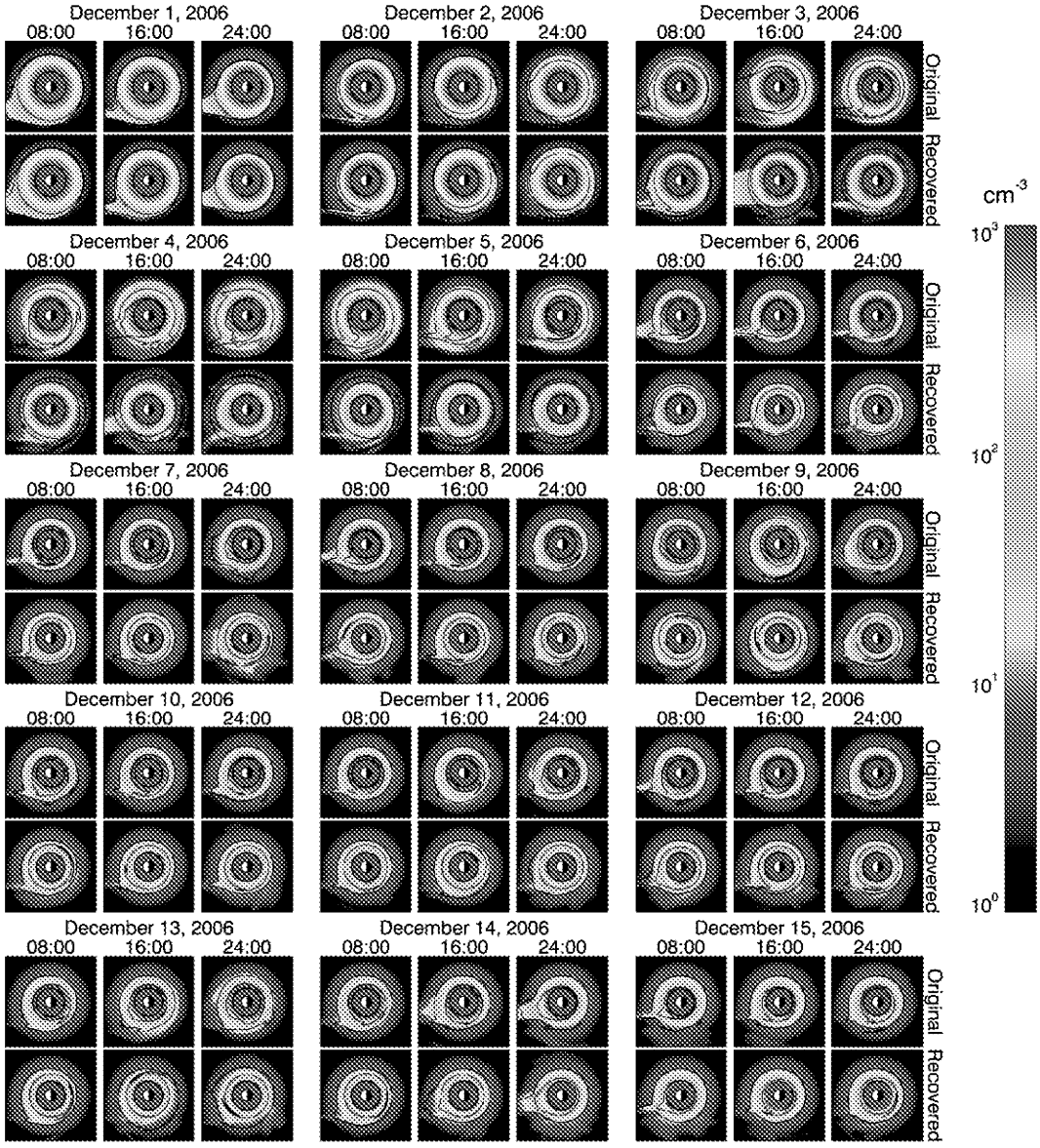

Fig. 7. Plasma density maps as a function of time for the first 15 days of December 2006. Each image is of a 16 by 16 R_E region centered on Earth with the sun at the left and dusk at the bottom. The color represents plasma density. Images are shown at 8 h intervals. (For interpretation of the references to colour in this figure legend, the reader is referred to the web version of this article.)

number of assimilation states, which is equivalent to increasing the search space for best solutions, has the effect of increasing the accuracy of the recovered plasma density and K_P values.

3.3. Geostationary or elliptical satellites?

In Fig. 9 we compare the effect of using only the elliptical orbit satellites and only the geostationary satellites to using all eight satellites. The three panels in this plot show K_P in the same format as described earlier. The top panel is the result of using all eight satellites, the center using only the four elliptical orbit satellites, and the bottom panel the result of using the four geostationary satellites. We expect that using more satellites will result in better performance. We also expect that using satellites which spend most of their time in regions where changes in K_P have a large effect on the measurements will result in better performance. It is clear that using only the four elliptical satellites results in a less accurate recovery of K_P (and also of plasma densities, not shown). In this particular case it also appears that using only the geostationary satellites outperforms using all eight satellites although that is less clear. One possible explanation for the better performance of the geostationary satellites in this case is the fact that K_P is small and therefore the plasmasphere extends to near geostationary orbit and exhibits significant structure there from which the data assimilation can be constrained. Under those same circumstances the elliptical orbit satellites will spend less time near the plasmapause and therefore provide much less

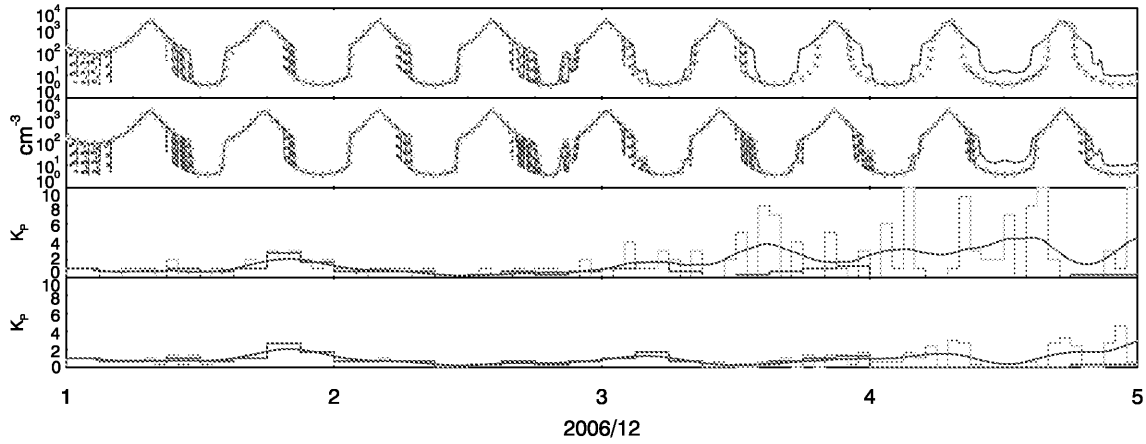

Fig. 8. Comparison of the effect of increasing the number parallel assimilation models, modeling the first 4 days of December 2006. The top two panels show plasma density measured by one satellite in the case 11 assimilation states (top panel) and 31 assimilation states (second panel). The corresponding K_P values are shown in the third and fourth panels respectively.

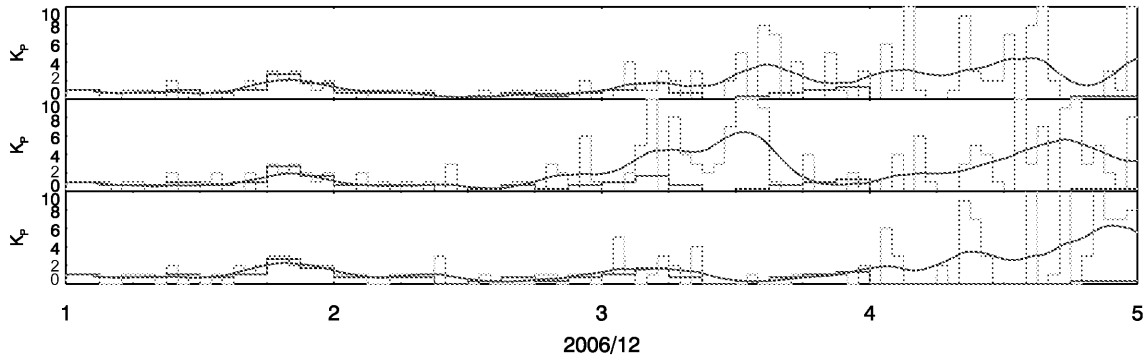

Fig. 9. Comparison of the effect of using all eight satellites (top panel) versus using only the elliptical orbit satellites (center panel) and only the geostationary orbit satellites (bottom panel).

constraint on the plasma density which is also seen from the less accurate recovered K_P values. The result which indicates that using only the geostationary satellites might produce a better model recovery than using all eight satellites is curious and may be a function of the specific choice of cost function, or of the effect proposed at the end of Section 3.1 of the satellites simply being in the wrong position and adding the weight of the elliptical satellites in the wrong position dominates the result.

4. Discussion

Overall the method succeeded in recovering the plasmasphere configuration and gross structure as well as the K_P index over most of the simulation interval. This is despite the simplicity of the data assimilation approach, and the fact that the model states available to the data assimilation did not match the states used to generate the input data.

It was also clear that increasing the number of simultaneous simulations, and thus the exhaustiveness of the search, resulted in better recovery of the plasma density and the K_P index values. This suggests that improving the data assimilation method will also result in improving the accuracy of the plasma density maps produced.

It is interesting to observe that despite the very wide swings observed in Fig. 5 in hourly K_P values, the plasma density is well modeled, and the average K_P still agrees well with the input K_P. This effect is particularly pronounced when we only allow the assimilation to use 11 states, whereas it is less pronounced when we allow the assimilation to use 31 states which more closely match the input K_P values, as is seen in Fig. 8. That figure shows that increasing the number of available assimilation states reduces the swings in the recovered K_P values and also results in a more accurately recovered plasma density. The reason for these wide swings are likely that the assimilation alternates between more eroding and less eroding plasmasphere models in order to, on average, approximate a state which is not available to the assimilation.

Concerning the distinction between elliptical and geostationary satellites, they sample different regions of the plasmasphere at different times. For example, during active times the geostationary satellites will be mostly outside the plasmasphere and not provide useful information except when they pass through the dayside or afternoon side

plume. Similarly, during quiet times the elliptical satellites sample primarily portions of the plasmasphere which do not vary with activity level, and therefore are not able to distinguish between different activity levels.

The poor agreement between input and recovered plasma density and K_P values on December 3–6 is somewhat puzzling. A likely reason for this is a "unlucky" situation with a sub-optimal placement of the satellites-in which they are not able to distinguish different drivers-combined with the selection of the wrong state from the small number available to the assimilation, which then takes the state further from the true state to the point where the assimilation cannot easily recover since it is forced to evolve according to the physics imposed by the Ober et al. (1997) model. This can also be seen clearly in Fig. 5: in the December 3–6 interval there are no blue traces which approach the red traces, thus indicating that the assimilation has accidentally entered a state from which there is no simple path back to agreeing with the data. The simple assimilation scheme we used in this paper does not include provisions for the data to force the plasma density when the model deviates too far from the data. Such provision are however contained in the Kalman filtering approach in which uncertainties in both the model and the data are accounted for. Of course this results in a model which does not evolve exactly according to the physical laws of the model. However given that the model is almost always an approximation to reality and that the primary goal is to accurately recover the configuration of the plasmasphere this should not be seen as a great loss. It can even be seen as an advantage in that data forcing of the model is an indicator of deficiencies in the model which can then be analyzed with the intent to improve the model (e.g Koller et al., 2007).

More data sources are available than the ones we simulated. Satellite measurements may not be the most powerful data sources for this work because of their single-point nature and the small number available. Exceptions might be the Los Alamos National Laboratory (LANL) geostationary satellites and their plasma instruments (Bame et al., 1993), as well as the GOES satellites. The LANL plasma density measurements may be used to identify plasmapause crossings, and possibly the distance to the plamasphere at other times. They may also be used to measure the magnetic field (Thomsen et al., 1996) to supplement the GOES magnetic field measurements. Over the next several years the Themis mission (Angelopoulos, 2008) can also be expected to be an interesting source of constraining data. In general any constraining data source can be included when it is available, and the decision as to its inclusion rests on the amount of effort involved in including it versus the benefits derived in constraining the model. Ground-based instruments are possibly more interesting sources of data because they often cover much larger regions of space than single satellites, because they are far less expensive to install and maintain, and because they usually persist for longer periods of time. These types of measurements include Field Line Resonance measurements (e.g. Schulz, 1996; Denton and Gallagher, 2000; Denton et al., 2009), which are now routinely carried out on data from the SAMBA, MEASURE, and McMac magnetometer chains (Boudouridis and Zesta, 2007; Berube et al., 2005). GPS TEC measurements have also been used to map space plasmas, both from the ground and from space (Belehaki et al., 2004; Yizengaw et al., 2008; Heise et al., 2002). Ground-based GPS measurements are greatly dominated by the ionosphere and provide limited useful information about the plasmasphere. Low-earth orbit measurements include the upper reaches of the ionosphere and the thermosphere, which must be correctly modeled in order that the measurements properly constrain the outer plasmasphere (e.g. Heise et al., 2002). Other information which can be included in the assimilation include whistler wave measurements (e.g. Lichtenberger, 2009), and improved models of the global magnetic field and global electric field, possibly also obtained using data assimilation approaches. Limited duration data sets in the past may not be helpful in constraining the plasmasphere for operational use today, but still have tremendous value in improving the models if the plasmasphere is densely sampled by those data sets. Examples include the four CLUSTER spacecraft and IMAGE EUV and RPI measurements (Darrouzet et al., 2009; Huang et al., 2004). The approach to using such data sources is to parametrize any new physics (for example a new description of the electric field), and then allow the assimilation to incorporate it.

5. Conclusion

We have demonstrated a simple approach to the assimilative modeling of the Earth's plasmasphere. Despite the simplicity of the data assimilation it performs well. We also demonstrated and discussed how the modeling scheme can be further improved both by improving the assimilation algorithm and by incorporating other data sources. Overall, this work demonstrates that assimilative modeling of the plasmasphere can be achieved with relatively simple tools and data sources.

References

Angelopoulos, V. The THEMIS mission. Space Sci. Rev. 141, 5–34, 2008.

Bame, S.J., McComas, D.J., Thomsen, M.F., Barraclough, B.L., Elphic, R.C., Glore, J.P., Gosling, J.T., Chavez, J.C., Evans, E.P., Wymer, F.J. Magnetospheric plasma analyzer for spacecraft with constrained resources. Rev. Sci. Instrum. 64, 1026–1033, 1993.

Belehaki, A., Jakowski, N., Reinisch, B.W. Plasmaspheric electron content derived from GPS TEC and digisonde ionograms. Adv. Space Res. 33, 833–837, 2004.

Berube, D., Moldwin, M.B., Fung, S.F., Green, J.L. A plasmaspheric mass density model and constraints on its heavy ion concentration. J. Geophys. Res. 110, A04212, 2005.

Boudouridis, A., Zesta, E. Comparison of Fourier and wavelet techniques in the determination of geomagnetic field line resonances. J. Geophys. Res. 112, A08205, 2007.

Darrouzet, F., De Keyser, J., Pierrard, V. (Eds.). The Earth's Plasmasphere: A CLUSTER and IMAGE Perspective. Springer, ISBN 978-1-4419-1322-7, p. 296, 2009.

Denton, R.E., Gallagher, D.L. Determining the mass density along magnetic field lines from toroidal eigenfrequencies. J. Geophys. Rev 105 (A12), 27717–27725, 2000.

Denton, R.E., Décréau, P., Engebretson, M.J., Darrouzet, F., Posch, J.L., Mouikis, C., Kistler, L.M., Cattell, C.A., Takahashi, K., Schäfer, S., Goldstein, J. Field line distribution of density at $L = 4.8$ inferred from observations by CLUSTER. Ann. Geophys., 27705–27724, 2009.

Evensen, G. The ensemble Kalman filter: theoretical formulation and practical implementation. Ocean Dyn. 52, 343–367, 2003.

Friedel, R.H.W., Reeves, G.D., Obara, T. Relativistic electron dynamics in the inner magnetosphere – a review. J. Atmos. Terr. Phys. 64, 265–282, 2002.

Heise, S., Jakowski, N., Wehrenpfennig, A., Reigber, Ch., Luehr, H. Sounding of the topside ionosphere/plasmasphere based on GPS measurements from CHAMP: initial results. Geophys. Res. Lett. 29 (14), doi:10.1029/2002GL014738, 2002.

Horne, R.B., Thorne, R.M. Potential waves for relativistic electron scattering and stochastic acceleration during magnetic storms. Geophys. Res. Lett. 25 (15), 3011–3014, 1998.

Huang, X., Reinisch, B.W., Song, P., Green, J.L., Gallagher, D.L. Developing an empirical density model of the plasmasphere using IMAGE/RPI observations. Adv. Space Res. 33 (6), 829–832, 2004.

Kalman, R.E. A new approach to linear filtering and prediction problems. J. Basic Eng. 82, 35–45, 1960.

Kalnay, E., Lord, S.J., McPherson, R.D. Maturity of operational numerical weather prediction: medium range. Bull. Am. Meteorol. Soc. 79, 2753–2892, 1998.

Koller, J., Friedel, R.H.W., Radiation belt diffusion parameter estimation with an adaptive Kalman filter, in: Presentation at AGU Fall Meeting 2005, SM12B-06, 2005.

Koller, J., Chen, Y., Reeves, G.D., Friedel, R.H.W., Cayton, T.E., Vrugt, J.A. Identifying the radiation belt source region by data assimilation. J. Geophys. Res. 112, A06244, 2007.

Kondrashov, D., Shprits, Y., Ghil, M., Thorne, R. A Kalman filter technique to estimate relativistic electron lifetimes in the outer radiation belt. J. Geophys. Res. 112, A10227, 2007.

Lemaire, J.F., Gringauz, K.I. The Earth's Plasmasphere. Cambridge University Press, Cambridge, 372 pp., 1998.

Lichtenberger, J. A new whistler inversion method. J. Geophys. Res. 114, A07222, doi:10.1029/2008JA013799, 2009.

Maget, V., Bourdarie, S., Boscher, D., Fridel, R.H.W. Data assimilation of LANL satellite data into the salammbo electron code over a complete solar cycle by direct inserting. Space Weather 5, S10003, 2007.

Naehr, S.M., Toffoletto, F.R. Radiation belt data assimilation with an extended Kalman filter. Space Weather 3, S06001, doi:10.1029/2004SW000121, 2005.

Ober, D.M., Horowitz, J.L., Gallagher, D.L. Formation of density troughs embedded in the outer plasmasphere by subauroral ion drift events. J. Geophys. Res. 102 (A7), 14595–14602, 1997.

Ramachandra, K.V. Kalman Filtering Techniques for Radar Tracking. CRC Press, 254 pp., 2000.

Rasmussen, C.E., Schunk, R.W. A three-dimensional time-dependent model of the plasmasphere. J. Geophys. Res. 95 (A5), 6133–6144, 1990.

Rasmussen, C.E., Guiter, S.M., Thomas, S.G. A two-dimensional model of the plasmasphere: refilling time constants. Planet. Space Sci. 41, 35–43, 1993.

Rigler, E.J., Baker, D.N., Weigel, R.S., Vassiliadis, D., Klimas, A.J. Adaptive linear prediction of radiation belt electrons using the Kalman filter. Space Weather 2, S03003, doi:10.1029/2003SW000036, 2004.

Schulz, M. Eigenfrequencies of geomagnetic field lines and implications for plasma-density modeling. J. Geophys. Res. 101 (A8), 17385–17397, 1996.

Sojka, J.J., Rasmussen, C.E., Schunk, R.W. An interplanetary magnetic field dependent model of the ionospheric convection electric field. J. Geophys. Res. 91 (A10), 11281–11290, 1986.

Thomsen, M.F., McComas, D.J., Reeves, G., Weiss, L. An observational test of the Tsyganenko (T89a) model of the magnetospheric field. J. Geophys. Res. 101 (A11), 24827–24836, 1996.

Yizengaw, E., Moldwin, M.B., Galvan, D., Iijima, B.A., Komjathy, A., Mannucci, A.J. Global plasmaspheric TEC and its relative contribution to GPS TEC. J. Atmos. Sol. Terr. Phys. 70, 1541–1548, 2008.